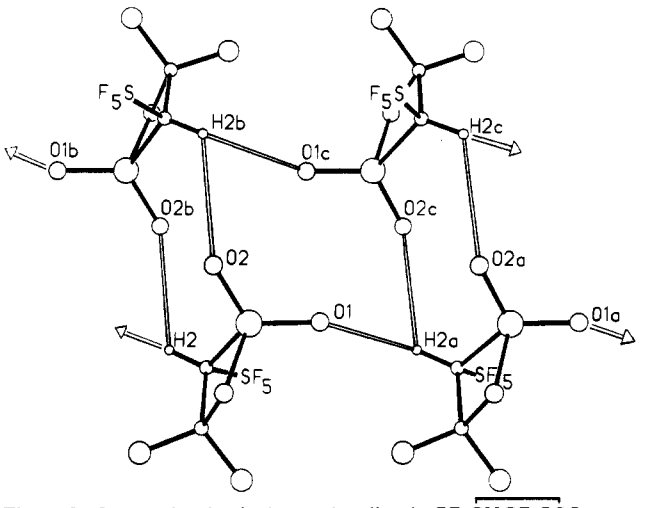

Figure 2. Intermolecular hydrogen bonding in $SF_5CHCF_2OSO_2$.

expected that these bond distances should decrease in going from the oxathietane (**1**) to the β-sultine (**2**) to the β-sultone (**3**) because of the increasing oxidation state of sulfur; this effect is seen in the shorter nonring SO bond distance for **3** versus **2**. A comparison of the bond angles for **1**–**3** shows good agreement for compounds **2** and **3**; for compound **1**, the bond angles were determined by assuming a planar four-membered ring. While compound **1** was assumed to be planar, compounds **2** and **3** are puckered with dihedral angles of 20.3[5] and (14.0, 13.7°), respectively. It is interesting to note that for perfluorocyclobutane a dihedral angle of 17.4° is found.[6] The values of the angles about sulfur, F-S(1)-F and C(2)-S(1)-F, correspond to a nearly octahedral arrangement of atoms bonded to S(1), with a maximum deviation of 2.9 (2)° in the F(2)-S(1)-F(3) angle (∠F-S-F = 177.1 (2)°).

Figure 2 shows a schematic ball and stick drawing of the intermolecular hydrogen bonding network of $SF_5CHCF_2OSO_2$. The C-H···O interactions are represented by open lines; those with arrowheads show interactions to neighboring, unpictured molecules. Lower case letters are used to distinguish symmetry-equivalent atoms. The hydrogen atom on one molecule forms a bifurcated interaction to a terminal oxygen atom on two other molecules. All hydrogen atoms and terminal oxygen atoms are therefore involved in intermolecular interactions. Several C-H···O interactions are shown in the figure, but only two are symmetry inequivalent: C(1)-H(2)···O(1)′ = 3.177 Å (∠C-H···O = 120.6°) and C(1)-H(2)···O(2)′ = 3.230 Å (∠C-H···O = 120.8°), where primes indicate atoms on neighboring molecules. These distances are long compared to normal interactions involving O-H and N-H groups (2.3 – 2.8 Å) but are comparable to the value of 3.2 Å reported for $(HCN)_n$.[7] There is little doubt that the hydrogen-bond network is responsible for the solid-state nature of $SF_5CHCF_2OSO_2$ at room temperature.

Experimental Section

The sultone $SF_5CHCF_2OSO_2$ was prepared according to the literature;[1] storage of the solid at room temperature under nitrogen at 1 atm resulted in formation of crystals acceptable for X-ray analysis. Examination of representative crystals under a polarizing microscope showed them to be optically biaxial but not sharply extinguishing.

Obtaining an acceptable X-ray data set was difficult due to the crystal quality problem mentioned above and also due to decomposition problems. When exposed to moisture, the crystals readily hydrolyze, and when exposed to pressures of less than an atmosphere at room temperature, they quickly sublime away. Sealed capillary methods were unsuccessful. More skillful drybox methods may have resolved the difficulties but were found to be unnecessary. Instead, an acceptable data set was obtained by using lower temperature techniques. A large crystal was cut by razor blade to a slightly larger than optimum size (≈0.8 mm cube). The crystal was attached by epoxy to a thin glass fiber and immersed in a -99 °C N_2 stream on a Nicolet R3m/E diffractometer system equipped with graphite-monochromated Cu Kα radiation. These steps were carried out under standard conditions but with haste (≈15 s). The resulting mounted crystal, nearly spherical in shape, 0.5 mm × 0.6 mm × 0.6 mm, was stable at the lowered temperature and showed no significant degradation during data collection. Peak scans showed the mounted crystal to be single-domain but to have very broad peak profiles. Subsequent Wycoff-ω data collection required peak scans of 2°.[8]

A total of 664 unique observed reflections, $|F_o| > 3\sigma(F_o)$ $\leq 2\theta \leq 100°$, were reduced to structure factor magnitudes by correction for Lorentz and polarization effects. Structure solution programs[9] led to resolution of all atomic positions. The hydrogen atom position was nevertheless constrained to C-H = 0.96 Å. All non-hydrogen atoms were refined anisotropically. The isotropic hydrogen atom thermal parameter was constrained to 1.2 times the equivalent isotropic parameter of the corresponding carbon atom. Crystal data are presented in Table I.

Acknowledgment. We wish to express our appreciation to the U.S. Department of Energy, Grant No. DE-FG21-88MC25142, for support of this work. The X-ray diffraction facility was established through funds from the NSF (Grant No. CHE-8404807) and the Boeing Co.

Supplementary Material Available: Full listings of data collection and refinement parameters, anisotropic thermal parameters, and hydrogen atom positions a unit cell packing diagram and (4 pages); a table of observed and calculated structure factors (4 pages). Ordering information is given on any current masthead page.

(6) Chang, C. H.; Porter, R. F.; Bauer, S. H. *J. Mol. Struct.* **1971**, *7*, 89.
(7) Dulmage, W. J.; Lipscomb, W. N. *Acta Crystallogr.* **1951**, *4*, 330.
(8) Campana, C. F.; Sheperd, D. F.; Litchman, W. N. *Inorg. Chem.* **1980**, *20*, 4039.
(9) Sheldrick, G. M. *SHELXTL Users Manual*, version 5.1; Nicolet Instrument Corp.: Madison, WI, 1986.

Contribution from the Departments of Chemistry, University of Minnesota, Minneapolis, Minnesota 55455, and Cornell University, Ithaca, New York 14853

Proton Nuclear Magnetic Resonance Studies of Iron(II/III)-Amide Complexes. Spectroscopic Models for Non-Heme Iron Proteins

Li-June Ming,† Randall B. Lauffer,‡ and Lawrence Que, Jr.*,†

Received October 25, 1989

Proton NMR spectroscopy has been a useful tool for investigating the metal binding site(s) of metalloproteins via the detection of the isotropically shifted proton signals.[1] While iron has successfully served as an intrinsic probe for the study of the active-site configuration of heme proteins and iron–sulfur proteins using several different NMR techniques,[1,2] its use as an NMR probe in other non-heme proteins is still not widely adopted and needs further exploration. The successful observation of isotropically shifted ^1H NMR signals of the iron-coordinated amino acid residues in the non-heme iron protein uteroferrin[3] has triggered studies on non-heme iron proteins by the use of NMR spectroscopy.[4] Features observed in the ^1H NMR spectrum of uteroferrin have been assigned to the histidyl imidazole protons and the tyrosyl protons.[3,5] Interestingly, an upfield-shifted solvent-exchangeable signal was also observed in the ^1H NMR spectrum that could not be assigned to an imidazole NH proton of a coordinated histidine residue[3,5] but could possibly arise from an NH proton of a peptidyl moiety coordinated through the carbonyl oxygen.[3,5] Alternatively, this signal may arise from a solvent-exchangeable proton in the proximity of the metal center upfield shifted via a dipolar shift mechanism.[1] In this paper, a

† University of Minnesota.
‡ Cornell University. Present address: NMR Section, Department of Radiology, Massachusetts General Hospital and Harvard Medical School, Boston, MA 02114.

0020-1669/90/1329-3060$02.50/0

^{1}H NMR study of simple iron–amide complexes (which may serve as models for amide binding in iron proteins) is presented in terms of the NH proton NMR chemical shifts and their relaxation properties.

Experimental Section

Materials. The complexes $[M(DAPSC)(Cl)(H_2O)]Cl\cdot 2H_2O$ (M = Fe^{2+}, Co^{2+})[6,7] and $Fe(FPSC)_2Cl_2$[8,9] were synthesized as previously described. The thio derivatives of $[Fe(DAPSC)Cl(H_2O)]^+$, i.e., $[Fe(DAPTSC)Cl(H_2O)]^+$ and its 4-methyl derivative, $[Fe(4\text{-}Me\text{-}DAPTSC)Cl(H_2O)]^+$, were prepared by following the same procedure as that for the DAPSC complexes using thiosemicarbazide or its 4-methyl derivative instead of semicarbazide in the condensation reaction. The structural similarity of the Fe^{2+}–thiosemicarbazone complexes to the Fe^{2+}–semicarbazone complex was demonstrated by ^{1}H NMR spectroscopy and relaxation measurements. $Fe(amide)_6(ClO_4)_3$ complexes were generated by the addition of the amide to $Fe(ClO_4)_3\cdot 6H_2O$ in acetone.

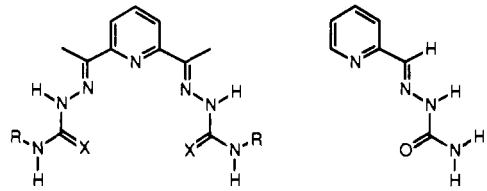

DAPSC: X=O, R=H
DAPTSC: X=S, R=H
4-Me-DAPTSC: X=S, R=Me

FPSC

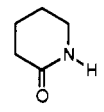

δ-valerolactam

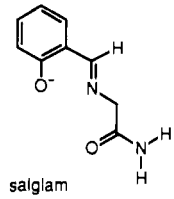

salglam

The complex $Fe(salglam)_2ClO_4$ was prepared as follows. To a solution of 1.79 g of glycinamide·HCl and 0.89 g NaOMe in 100 mL of absolute methanol over low heat was added 1.97 g of salicylaldehyde forming a yellow solution. A 2.94-g amount of $Fe(ClO_4)_3\cdot 6H_2O$ in 20 mL of absolute ethanol was added to the solution to form a purple mixture that was cooled and the NaCl separated by filtration. A hot 3:1 toluene: acetonitrile solution (~300 mL) was used to precipitate 3.0 g (74%) of the crude complex, which was recrystallized from absolute ethanol. Anal. Calcd for $Fe(salglam)_2ClO_4\cdot 0.5C_2H_5OH$: C, 42.64; H, 4.01; N, 10.52. Found: C, 42.43; H, 4.21; N, 10.29.

Physical Measurements. ^{1}H and ^{2}H NMR spectra of the complexes were obtained on Bruker WM300 (300 MHz for ^{1}H and 46 MHz for ^{2}H) and IBM NR/300 (300 MHz) spectrometers. Single 90° pulses (ca. 10 μs) were employed for taking the ^{1}H NMR spectra with 8K data points and a sufficiently large spectral width to cover all the isotropically shifted signals. The signal-to-noise ratio of the spectra was improved by an exponential multiplication of the FID's to introduce an additional 5–30-Hz line broadening. ^{2}H NMR spectra were obtained by using 90° (30 μs) pulses with a 15-kHz spectral width and 4K data points and around 100 000 transients. ^{1}H NMR spin–lattice relaxation times (T_1) of signals without chemical exchange were obtained with the standard inversion-recovery method. The validity of the measurements was checked by varying the carrier frequency. Owing to the relatively long pulse (ca. 10 μs/90°), a simultaneous inversion of all the isotropically shifted signals (which are spread over 40 kHz at 300 MHz) is impossible, and a pseudoselective excitation of the resonance at the carrier frequency is observed. Because of the inefficiency of the rf pulse, along with the chemical exchange of the two amide NH_2 protons caused by rotation of the amide C–N partial double bond (which allows the observation of two well-resolved amide NH_2 resonances),[10] an accurate measurement of the relaxation times of the two amide NH_2 protons in the iron complexes by the inversion-recovery method is not straightforward. A shorter relaxation time for an NH signal would be expected when the carrier frequency is set closer to the signal, since the magnetization of its geminal NH proton (which is more than 20 kHz away) is poorly inverted and may serve as a good relaxation pool for the inverted signal to relax. However, a saturation-transfer experiment using a modified Bloch equation that includes the chemical exchange term[11] gives reliable estimates for the relaxation times (see below).

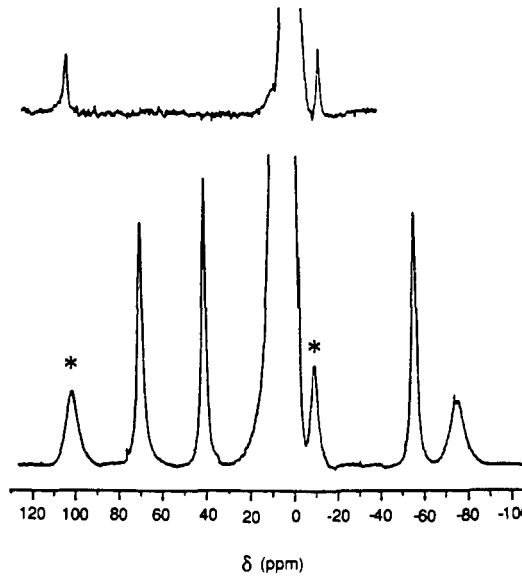

Figure 1. ^{1}H NMR spectrum (300 MHz) of $Fe^{III}(salglam)_2ClO_4$ in acetone-d_6 at 323 K. The exchangeable signals are marked by asterisks. The inset is the ^{2}H NMR spectrum (46 MHz) of this complex in acetone-d_6 with one drop of D_2O at 303 K.

Saturation-transfer experiments were performed by setting the decoupling pulse on one of the amide NH_2 signals with sufficient power to saturate the signal in a short duration time ($t \leq 5$ ms). A transfer of the magnetization from the saturated signal of one of the amide NH_2 protons to the other may occur to different extents, depending upon the rate constant of the amide C–N bond rotation and the relaxation times of the NH_2 protons. When two sites A and B are chemically exchangeable, the Bloch equation can be modified[11] to include the chemical exchange, as shown in eq 1 for resonance A if resonance B is assumed to be saturated

$$dM_z^A/dt = M_0^A/T_{1A} - M_z^A/\tau_{1A} \quad (1)$$

instantaneously, where $1/\tau_{1A} = 1/T_{1A} + 1/\tau_A$, T_{1A} is the relaxation time of resonance A, and τ_A is the lifetime in site A. A similar equation can also be obtained for B. In the case of the rotation of the amide C–NH_2

(1) Bertini, I.; Luchinat, C. *NMR of Paramagnetic Molecules in Biological Systems*; Benjamin/Cummings: Menlo Park, CA, 1986.
(2) Satterlee, J. D. In *Metal Ions in Biological Systems*; Sigel, H., Ed.; Dekker: New York, 1987; Vol. 21, Chapter 4.
(3) Lauffer, R. B.; Antanaitis, B. C.; Aisen, P.; Que, L., Jr. *J. Biol. Chem.* **1983**, *258*, 14212–14218.
(4) Que, L., Jr.; Scarrow, R. C. In *Metal Clusters in Proteins*; Que, L., Jr., Ed.; ACS Symposium Series 372; American Chemical Society: Washington, DC, 1988; Chapter 8.
(5) Scarrow, R. C.; Pyrz, J. W.; Que, L., Jr. *J. Am. Chem. Soc.* **1990**, *112*, 657–665.
(6) Abbreviations: DAPSC, 2,6-diacetylpyridine bis(semicarbazone); DAPTSC, DAP bis(thiosemicarbazone); DMA, *N,N*-dimethylacetamide; DMF, *N,N*-dimethylformamide; FID, free induction decay; FPSC, 2-formylpyridine semicarbazone; rf, radio frequency; salglam, N^{α}-salicylideneglycinamide; SOD, superoxide dismutase; HiPIP, high-potential iron protein.
(7) Palenik, G. J.; Wester, D. W. *Inorg. Chem.* **1978**, *17*, 864–870.
(8) The complexes $M(FPSC)_2Cl_2$ (1:2 complex) and its derivatives are well-known to be cytotoxic and are used for tumor therapeutic studies.[9] The 1:2 Fe(II) complex is diamagnetic, as shown by the observation of well-shaped ^{1}H NMR signals in the diamagnetic region; however, the 1:1 complex is paramagnetic, showing isotropically shifted ^{1}H NMR signals spread over 200 ppm (Table I).
(9) (a) Agrawal, K. C.; Booth, B. A.; Michaud, R. L.; Moore, E. C.; Sartorelli, A. C. *Biochem. Pharmacol.* **1974**, *23*, 2421–2429. (b) Antholine, W. E.; Knight, J. M.; Petering, D. H. *J. Med. Chem.* **1976**, *19*, 339–341. (c) Antholine, W. E.; Knight, J. M.; Petering, D. H. *Inorg. Chem.* **1977**, *16*, 569–574.
(10) (a) Redfield, A. G.; Waelder, S. *J. Am. Chem. Soc.* **1979**, *101*, 6151–6162. (b) Perrin, C. L.; Johnston, E. R.; Lollo, C. P.; Kobrin, P. A. *J. Am. Chem. Soc.* **1981**, *103*, 4691–4696. (c) Perrin, C. L.; Johnston, E. R. *J. Am. Chem. Soc.* **1981**, *103*, 4697–4703. (d) Krishna, N. R.; Sarathy, K. P.; Huang, D.-H.; Stephens, R. L.; Glickson, J. D.; Smith, C. W.; Walter, R. *J. Am. Chem. Soc.* **1982**, *104*, 5051–5053.
(11) (a) Forsén, S.; Hoffman, R. A. *Acta Chem. Scand.* **1963**, *17*, 1787–1788. (b) Forsén, S.; Hoffman, R. A. *J. Chem. Phys.* **1963**, *39*, 2892–2901. (c) McConnell, H. M. *J. Chem. Phys.* **1958**, *28*, 430–431.

Table I. ^{1}H NMR Chemical Shifts of Amide Complexes at 300 K

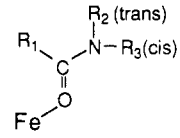

compound	chemical shift, ppm R_1	R_2	R_3	other
$[Fe^{III}(amide)_6]^{3+a,b}$				
acetamide	(27)	63	−30	
N-methylacetamide		86	(58)[c]	
N,*N*-dimethylacetamide (DMA)		(67)	(50)[c]	
N,*N*-dimethylformamide (DMF)		(62)	(51)	
δ-valerolactam	(24)	(97)[c]	−36	
$Fe^{III}(salglam)_2ClO_4$[a]		111	−10	3-H, −81; 4-H, 77; 5-H, −60; 6-H, 45
$[Fe^{II}(DAPSC)(Cl)(H_2O)]Cl$[d]	112.9[e]	56.2	−8.8	*m*-H, 55.1; *p*-H, 13.0; Me, −22.3
$[Fe^{II}(DAPTSC)(Cl)(H_2O)]Cl$[d]	109.3[e]	75.8	−8.2	*m*-H, 51.1; *p*-H, 16.7; Me, −15.5
$[Fe^{II}(4\text{-Me-DAPTSC})(Cl)(H_2O)]Cl$[b,d]	107.6[e]	36.5	(6.5)	*m*-H, 52.0; p-H, 15.3; Me, −15.5
$Fe^{II}(FPSC)Cl_2$[d]	155.2[e]	90.4	22.8	*m*-H, 55.2, 30.0; *p*-H, 22.8; *o*-H, 202; CH, 177.7
$[Co^{II}(DAPSC)(Cl)(H_2O)]Cl$[d]	175.5[e]	85.8	31.3	*m*-H, 86.4; *p*-H, 24.2

[a] In acetone-d_6. [b] Values in parentheses indicate methyl or methylene protons. [c] Alternatively, the signal may arise from the O=C—methyl (methylene) protons; however, its being assigned to the R_3 methyl group is more consistent with that observed in the DMF complex. [d] In DMSO-d_6. [e] N–NH proton.

bond, the lifetimes of the NH_2 protons in each site are equal, i.e. $\tau_A = \tau_B$. If the resonance at site B is saturated instantaneously at time $t = 0$ (i.e., when $M_z^A = M_0^A$), the decay of M_z^A with the irradiation duration time t can be obtained by solving eq 1 to give eq 2.[11]

$$M_z^A = M_0^A[(\tau_{1A}/\tau_A)\exp(-t/\tau_{1A}) + (\tau_{1A}/T_{1A})] \quad (2)$$

In the case of fast chemical exchange between the two sites, along with the very short relaxation times of paramagnetic species, a plot of $\ln [M_z^A - (\tau_{1A}/T_{1A})M_0^A]$ versus t giving the slope of $-1/\tau_{1A}$ is not practically obtainable. However, under the saturation condition of $t \rightarrow \infty$ on signal B, the magnetization of signal A becomes as in eq 3, and the value of τ_{1A}

$$M_z^A(t\rightarrow\infty) = M_0^A(\tau_{1A}/T_{1A}) \quad (3)$$

can be obtained as $T_{1A}[M_z^A(t\rightarrow\infty)/M_0^A]$. From eqs 1–3 for both resonances A and B, a ratio of T_{1A}/T_{1B} can be calculated, and distance information can be therefore obtained by applying the Solomon equation in which the relaxation rates (T_1^{-1}) are directly proportional to the negative sixth power of the distance between the nucleus and the paramagnetic center (r^{-6}).[12]

Results and Discussion

Ferric–Amide Complexes. The NMR spectra of amides in general show two NH signals due to the restricted rotation (activation barrier of about 20 kcal/mol[13]) about the C–N partial double bond.[10,13] The ^{1}H NMR spectra of a series of iron–amide complexes we have studied indicate that the ligation of the iron presumably through the carbonyl oxygen[14] also gives rise to inequivalent amide NH_2 protons, but in the metal complexes the two protons are usually distinguished by being shifted in opposite directions. The ^{1}H NMR spectrum of $[Fe(salglam)_2]ClO_4$ in acetone-d_6 at 50 °C (Figure 1) exhibits two solvent-exchangeable NH signals at −8.9 and 103 ppm; these assignments are confirmed by ^{2}H NMR observations on the same solution (at 30 °C) but with one drop of D_2O to exchange the NH_2 protons with deuterium (Figure 1, inset). Similarly, $Fe(acetamide)_6(ClO_4)_3$, presumed to be octahedral by analogy to the crystallographically characterized $Fe(DMF)_6(ClO_4)_3$ and $Fe(urea)_6(ClO_4)_3$ complexes,[14] exhibits two solvent-exchangeable signals at 63 and −30 ppm (Table I), which are broad due to the long T_{1e} of the complex engendered by its high symmetry.[15]

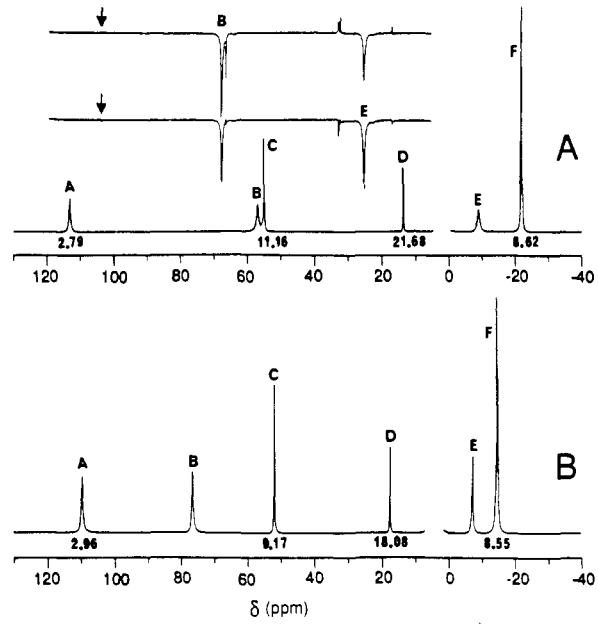

Figure 2. ^{1}H NMR spectra of (A) $[Fe^{II}(DAPSC)(Cl)(H_2O)]Cl$ and (B) $[Fe^{II}(DAPTSC)(Cl)(H_2O)]Cl$ in DMSO-d_6 at 300 K. The resonances A, B, and E are solvent exchangeable signals, which disappear with one drop of D_2O in DMSO-d_6. T_1 values (ms) of the isotropically shifted signals are also shown (for those of signals B and E, see text). The inset in part A shows the results of the saturation transfer experiments where the saturation pulse is set on signal B (top) or on signal E (bottom). The arrows indicate the positions of signal A showing no saturation-transfer effect.

The two amide NH_2 protons can be identified as being either trans (H_t) or cis (H_c) to the carbonyl oxygen with the shorter Fe–H distance for the cis proton[7] (see structure in Table I). In the *N*-methylacetamide complex where the H_c proton is replaced by a methyl group,[16] the only NH signal is observed at 86 ppm (Table I), which therefore may be assigned to the trans proton. On the other hand, the δ-valerolactam complex, in which the H_t proton is replaced by a methylene group, shows only one NH signal at −36 ppm (Table I). These observations indicate that the upfield- and downfield-shifted solvent-exchangeable signals of an iron(III)–amide complex may be due to the H_c and H_t protons, re-

(12) Solomon, I. *Phys. Rev.* **1955**, *99*, 559–565.
(13) Steward, W. E.; Siddall, T. H., III. *Chem. Rev.* **1970**, *70*, 517–551.
(14) (a) Sumner, R. H. Ph.D. Thesis, University of Alberta, 1971. (b) Holt, E. M.; Alcock, N. W.; Sumner, R. H.; Asplund, R. O. *Cryst. Struct. Commun.* **1979**, *8*, 255–259. (c) Calogero, S.; Russo, U.; Del Pra, A. *J. Chem. Soc., Dalton Trans.* **1980**, 646–653.
(15) La Mar, G. N.; Walker, F. A. *J. Am. Chem. Soc.* **1973**, *95*, 6950–6956.
(16) Davies, D. B.; Khaled, M. A. *J. Chem. Soc., Perkin Trans. 2* **1973**, 1651–1655.

spectively. When both NH_2 protons are replaced by methyl groups as in the DMF and DMA complexes, only downfield resonances are detected (Table I). T_1 values of 0.73 and 0.35 ms were obtained for the methyl signals at 62 and 51 ppm, respectively, in the DMF complex, indicating that the latter one corresponds to the cis methyl group.

Ferrous–Amide Complexes. The ^1H NMR spectrum of the pentagonal-bipyramidal[7] complex [Fe(DAPSC)Cl(H_2O)]Cl shows three solvent-exchangeable signals (Figure 2A). Ferrous complexes, in general, exhibit much sharper signals due to the fast electronic relaxation rate of the ferrous ion.[1] Saturation of either signal B or signal E causes substantial saturation transfer (>70%) to each other (but not to signal A), indicating that the two signals at 56.2 and −8.8 ppm are due to the amide NH_2 protons, while that at 112.9 ppm arises from the N–NH proton (Figure 2A, inset). The assignments of the amide NH_2 protons can in principle be determined by measuring the relaxation rates of the two protons according to the Solomon equation.[12] However, the relaxation times of these two protons cannot be determined accurately owing to the presence of the chemical exchange and the inefficiency of the rf pulse used (cf. Experimental Section). T_1 values of 5.13 and 8.67 ms were obtained for signal B by using the inversion-recovery measurement with the carrier frequency set on signal B and on signal E, respectively. Corresponding values for signal E were 4.28 and 7.93 ms when the carrier frequency was set on E and on B, respectively. Similarly, values of 9.51 and 14.62 ms were obtained for signal B (7.29 and 11.38 ms for signal E) of the DAPTSC complex (Figure 2B) with the carrier frequency set on signals B and E (on E and B), respectively. The values of 5.13 ms (or 195 s^{-1}) and 4.28 ms (or 234 s^{-1}) for B and E, respectively, of the DAPSC complex are close to the values obtained by selective T_1 measurements (229 and 249 s^{-1}, respectively) using small excitation windows. This observation indicates that the smaller T_1 values obtained by setting the carrier frequency on the signals do arise from pseudoselective excitation of the signals, as mentioned in the Experimental Section. These relaxation data are thus not useful for correlating the ^1H NMR spectra to the geometric configuration of the iron complexes.

However, saturation-transfer experiments provide a more reliable assignment for the amide NH_2 features. A ratio of the magnetization of signal B relative to its static magnetization (i.e., M_z/M_0) of 18.0 ± 2% was observed when signal E was completely saturated for >100 ms in the DAPSC complex, and a value of 27.4 ± 1% was observed for signal E when B was saturated. An average $(T_{1B}^{-1}/T_{1E}^{-1})^{-1/6}$ value of 1.10 ± 0.04, which is proportional to (r_{M-B}/r_{M-E}),[12] can be obtained according to eqs 1–3. This result is in agreement with the crystallographic studies that afforded a value of 1.094 for (r_{M-H_t}/r_{M-H_c}).[17] Thus, signal B is associated with the trans proton and signal E is assigned to the cis proton of the amide. Similarly, ratios of 74.1 ± 2.3% and 80.6 ± 3.8% were obtained for signals B and E, respectively, in the DAPTSC complex, which yielded a value of $(T_{1B}^{-1}/T_{1E}^{-1})^{-1/6}$ of 1.07 ± 0.07. The smaller saturation transfer of the magnetization between the amide NH_2 protons of the DAPTSC complex indicates a more rigid C–N partial double bond, which may produce a smaller kinetic perturbation on the relaxation rates of the amide NH_2 protons as mentioned before. Indeed, a smaller variation in T_1^{-1} (ΔT_1^{-1} = 37 s^{-1}) was obtained for signal B relative to that of the DAPSC complex (ΔT_1^{-1} = 114 s^{-1}) when nonselective versus selective T_1 measurements were used. The 4-methylthiosemicarbazone (4-Me-DAPTSC) complex shows only one amide NH signal (Table I), which is downfield shifted and has a relaxation rate of T_{1NH}^{-1} = 96 s^{-1}; this value is close to that of the acetyl methyl protons (signal F, $(T_{1NH}^{-1}/T_{1F}^{-1})^{-1/6}$ = 1.04), which has an M–H distance similar to the M–H_t distance in the DAPSC complex (r_{M-H_t}/r_{M-F} = 1.001 while r_{M-H_c}/r_{M-F} = 0.915).[17,18]

These results strongly suggest that the upfield-shifted NH proton (signal E) in these iron–amide complexes is due to the cis amide proton, and the downfield-shifted NH resonance (signal B) is due to the trans amide proton.

The ^1H NMR spectrum of the complex Fe(FPSC)Cl_2 shows only downfield-shifted signals with the two amide NH_2 protons isotropically shifted to 90.4 and 22.8 ppm (Table I). The assignment of the two NH_2 protons in this complex can be confirmed by the saturation-transfer experiment. Interestingly, the complex Co[(DAPSC)Cl(H_2O)]Cl with a structure very similar to its iron analogue[7] also shows two NH signals isotropically shifted to the downfield region at 86.1 and 31.6 ppm (confirmed by deuterium exchange and saturation transfer).

Amide NH_2 Shift Patterns. While the origins of the two well-separated ^1H NMR signals of the NH_2 protons in primary amides are well studied and understood,[10,13] the detection of two NH signals with chemical shifts in opposite directions for the Fe–amide complexes is unprecedented. In paramagnetic complexes, the Fermi contact interaction between unpaired electrons and nuclei on the ligand (via σ spin delocalization) engenders the observation of downfield-shifted signals in most cases.[1,19] Indeed the fact that the trans NH and the trans N–CH_3 protons both shift downfield suggests that the trans NH proton is shifted predominantly via the σ spin delocalization. The observation of upfield-shifted cis NH signals in the Fe–amide complexes, however, suggests the participation of dipolar shift, spin polarization (e.g., with the configuration $\uparrow O\uparrow\downarrow C\downarrow\uparrow N\uparrow\downarrow H$), or π spin delocalization mechanisms for the cis NH protons.[1,19] The opposite shift observed upon methyl substitution for the cis NH proton (with the configuration $\uparrow O\uparrow\downarrow C\downarrow\uparrow N\uparrow\downarrow C\downarrow\uparrow H$), as shown in the DMF, DMA, and 4-Me-DAPTSC complexes (Table I), is consistent with the involvement of either spin polarization or π spin delocalization mechanisms. (The dipolar mechanism can be ruled out in high-spin Fe(III) complexes owing to their ^6S ground states.)

Why are the two NH protons affected differently by the metal center? Both spin polarization and spin delocalization mechanisms would be expected to affect the two amide NH_2 protons similarly if the C–N bond were freely rotating, since they are both four-bond distant from the iron center. However, under the conditions of restricted C—N rotation, the two NH_2 protons have different orientations with respect to the C=O moiety. On the basis of the crystal structures of the DAPSC complexes,[7,17] the cis NH proton is out of the O=C—N plane by ~11.1°, while the trans NH proton is nearly in the plane (~2.5°). The negative spin density on the amide C–p_π orbital would therefore be more efficiently transmitted to the cis NH proton via hyperconjugation,[19] resulting in a shift opposite to that due to σ delocalization. In most cases (except for the FPSC complex), this effect is apparently large enough to engender an upfield shift. Similar differences in shifts are observed for conformationally restricted geminal protons in many simple metal complexes and proteins.[5,19,20] For ferrous complexes the magnetic anisotropy in the ferrous center may also shift the two NH_2 signals in different directions by the dipolar mechanism because the two NH_2 protons have opposite signs for the $1 - 3\cos^2\theta$ factor, assuming that the complex is axially symmetric with $\chi_\parallel$ along the Fe–N(pyridine) bond.[7]

On the basis of the present results on a limited number of complexes, the upfield-shifted solvent-exchangeable feature in the ^1H NMR spectrum of uteroferrin cannot be readily associated with the NH proton of a coordinated amide carbonyl. The peptidyl NH protons in proteins are nearly always trans to the carbonyl oxygen forming the rigid planar O=C—N—H peptide unit[21] and

(17) The M–H distances used here are based on the crystallographic data of the manganese complex in which all the proton coordinates were given.[7] We have assumed that the structure and the proton configuration of the iron complexes are similar to those of the manganese complex.[7]

(18) By comparing the observed relaxation rates of the amide NH_2 protons of the DAPTSC complex to those of the DAPSC complex, those of the former ones are clearly smaller (larger r_{Fe-H}) than those of the latter ones while those of the other protons are very similar (Figure 2). When this is taken into account, the value of $(T_{1NH}^{-1}/T_{1F}^{-1})^{-1/6}$ of the amide NH signal in the 4-Me-DAPTSC complex is still closer to the r_{M-H_t}/r_{M-F} value of the trans proton in the DAPTSC complex.

(19) La Mar, G. N. In *NMR of Paramagnetic Molecules. Principles and Applications*; La Mar, G. N., Horrocks, W. D., Jr.; Holm, R. H., Eds.; Academic: New York, 1973.

(20) Holm, R. H.; Hawkins, C. J. In ref 19, Chapter 7.

would thus be shifted downfield when coordinated to an iron center, while amide protons on glutamine and asparagine coordinated via the amide carbonyl are expected to have one upfield and one downfield signal. The downfield solvent-exchangeable features of uteroferrin are currently assigned to imidazole NH's on histidines coordinated to either Fe(III) or Fe(II) of the dinuclear site because their chemical shifts match well with those expected of histidine coordination.[22] At present, imidazole is a more likely ligand for iron in uteroferrin and amide ligation appears unlikely. Upfield-shifted solvent-exchangeable resonances are also observed in the ^{1}H NMR spectra of yeast Cu,Co-SOD (−25.1 ppm)[23] and HiPIP's from *Rhodospirillum tenue* (−5.4 and −9.6 ppm)[24] and *Chromatium gracile* (−8.0 and −19.2 ppm);[25] these protons are associated with NH protons that are in the close proximity of the magnetically anisotropic metal centers. A similar assignment may be appropriate for the upfield-shifted solvent-exchangeable feature in uteroferrin, but OH protons that are slow to exchange are also possible candidates.

Acknowledgment. This work was supported by the National Institutes of Health (Grant GM-33162).

(21) Schulz, G. E.; Schirmer, R. H. *Principles of Protein Structure*; Springer-Verlag: New York, 1979.

(22) (a) Maroney, M. J.; Kurtz, D. M., Jr.; Nocek, J. M.; Pearce, L. L.; Que, L., Jr. *J. Am. Chem. Soc.* **1986**, *108*, 6871–6879. (b) Pillai, R. P.; Lenkinski, R. E.; Sakai, T. T.; Geckle, J. M.; Krishna, N. R.; Glickson, J. D. *Biochem. Biophys. Res. Commun.* **1980**, *96*, 341–349. (c) Balch, A. L.; Chan, Y.-W.; LaMar, G. N.; Latos-Grazynski, L.; Renner, M. W. *Inorg. Chem.* **1985**, *24*, 1437–1443. (d) Goff, H.; LaMar, G. N. *J. Am. Chem. Soc.* **1977**, *99*, 6599–6606. (e) Wu, F.-J.; Kurtz, D. M., Jr. *J. Am. Chem. Soc.* **1989**, *111*, 6563–6572.

(23) Ming, L.-J.; Banci, L.; Luchinat, C.; Bertini, I.; Valentine, J. S. *Inorg. Chem.* **1988**, *27*, 728–733.

(24) Krishnamoorthi, R.; Cusanovich, M. A.; Meyer, T. E.; Przysiecki, C. T. *Eur. J. Biochem.* **1989**, *181*, 81–85.

(25) Sola, M.; Cowan, J. A.; Gray, H. B. *Biochemistry* **1989**, *28*, 5261–5268.